

1

Submitted to *Journal of Oceanography*

2

Variation of the southward interior flow of the North Pacific subtropical

3

gyre, as revealed by a repeat hydrographic survey

4

Keywords: North Pacific, Subtropical gyre, Interior region, Volume transport, Volume

5

transport-averaged temperature

6

7

Akira Nagano^{*,1}, Hiroshi Ichikawa¹, Yasushi Yoshikawa², Shoichi Kizu³,

8

and Kimio Hanawa³

9

¹ Research Institute for Global Change, Japan Agency for Marine-Earth Science and

10

Technology, 2-15 Natsushima-cho, Yokosuka, Kanagawa 237-0061, Japan

11

² Mutsu Institute for Oceanography, Japan Agency for Marine-Earth Science and Technology

12

³ Graduate School of Science, Tohoku University

13

*Corresponding author. Japan Agency for Marine-Earth Science and Technology,

14

2-15 Natsushima-cho, Yokosuka, Kanagawa 237-0061, Japan

15

E-mail: nagano@jamstec.go.jp

16

Phone: +81-46-867-9846, Fax: +81-46-867-9455

17

Abstract

Baroclinic variations of the southward flow in the interior region of the North Pacific subtropical gyre are presented with five hydrographic sections from San Francisco to near Japan during 2004–2006. The volume transport-averaged temperature of the interior flow, which varies vigorously in the range of 0.8°C , is negatively correlated with the transport in the density layer of $24.5\text{--}26.5\sigma_{\theta}$, associated with the vertical current structure changes. The transport variation in the density layer is thus mainly responsible for the thermal impact of the interior flow on the heat transport of the subtropical gyre.

1 Introduction

The subtropical gyre of the North Pacific transports considerable amount of heat from the tropical region to the mid-latitude region. Since its net meridional heat transport is considered to play a critical role in the global climate system, many investigators have conducted its estimation in past (Bryden and Imawaki, 2001; Nagano et al., 2009, 2010). To estimate the net heat transport of the subtropical gyre, volume transport-averaged temperatures of currents involved in the gyre have been frequently used in past studies such as Nagano et al. (2009, 2010); thus, the volume transport-averaged temperatures are essential indices to evaluate the thermal impacts of the current variations on the climate.

Except the region of the northeastward flowing western boundary current, so-called the Kuroshio, most part of the subtropical gyre is occupied with the southward flow. The southward interior flow constitutes the return flow of the Kuroshio, i.e., the western boundary current of the North Pacific subtropical gyre. The volume transport-averaged temperature in the interior region, T_1 , is lower than that of the Kuroshio due to the intensive heat loss from the sea surface

40 in the Kuroshio Extension region, east of Japan. In comparison with the volume transport-
41 averaged temperature of the Kuroshio, T_1 has not been studied intensively because of too long
42 ship time necessary for and then rare occasions of trans-Pacific observations.

43 A trans-Pacific hydrographic section of the World Ocean Circulation Experiment (WOCE)
44 P02, at the latitude of 30°N, was obtained in parts by two cruises in October 1993 and January
45 1994. From this data, Bryden and Imawaki (2001) calculated T_1 to be 15.8°C. From another data
46 of the P02 observation in June–August 2004, Nagano et al. (2009) calculated T_1 to be 15.4°C.
47 Taking into account of the variations of the volume transport and the volume transport-averaged
48 temperature of the Kuroshio, Nagano et al. (2010) calculated the meridional heat transport of the
49 subtropical gyre to be 0.19–0.22 PW (1 PW = 10^{15} W) by the use of 15.4°C as T_1 . Nagano et al.
50 (2010) noted that the use of 15.8°C instead of 15.4°C reduces about 20% of the net heat transport
51 of the gyre. Thus, only such an overestimation of T_1 results in a significant underestimation of
52 the net heat transport of the subtropical gyre.

53 Because of insufficient knowledge on the variation of T_1 , Bryden and Imawaki (2001) and
54 Nagano et al. (2009, 2010) assumed T_1 to be constant. For more accurate estimation of the
55 heat transport, we should examine the variability of the flow and thermal structures which are
56 associated with the variation of T_1 . By using expendable bathythermograph (XBT) and/or
57 conductivity-temperature-depth (XCTD) probes, repeat high-resolution XBT/XCTD (HRX)
58 data have been collected along cruise tracks of voluntary ships in the North Pacific (e.g., Roem-
59 mich et al., 2001; Uehara et al., 2008) and other oceans. The HRX data can supplement the
60 trans-Pacific data at the WOCE hydrographic lines such as P02, and the analysis of the HRX
61 data is expected to reveal the variations of the flow and thermal structures in the interior region
62 of the subtropical gyre.

63 In this paper, we calculated T_1 from five sets of hydrographic sections from Honolulu
64 (Hawaii) to San Francisco (California) (HRX-PX37) by the M/V *Enterprise* and from Hon-
65 olulu to Japan (PX40) by the T/V *Miyagi-maru* in June 2004–November 2006 since the five
66 sections were collected almost simultaneously in the interior region of the subtropical gyre.

67 **2 Data**

68 The line of PX40 largely intersects a western part of the interior region of the subtropical gyre at
69 an average latitude of about 29°N (Fig. 1). Detailed information about the cruises along the line
70 of PX40 was provided by Uehara et al. (2008). From 150°E to Japan, the *Miyagi-maru* took the
71 northern or southern routes which were oriented to the ports in Miyagi or Kanagawa prefectures,
72 respectively. The deviations of the cruise tracks in the Kuroshio Extension region may cause
73 large errors of the estimated values of the volume transport and volume transport-averaged
74 temperature due to abrupt and complicated spatial variations of the current there. Thus, we
75 used the data east of 150°E where the tracks deviated less than 3° from the latitude of the mean
76 track and did not intersect the Kuroshio Extension.

77 Temperature data at PX40 were obtained almost three times a year in March, June, and
78 November down to a depth of about 780 m at the longitudinal interval of 0.5° by XBT T-7
79 probes (The Tsurumi-Seiki Co., Ltd.) which are rated to 760 m depth. The salinity at each
80 XBT site was estimated from the temperature-salinity relationship at the nearest XCTD site at
81 the longitudinal interval of 5° by XCTD-1 probes (The Tsurumi-Seiki Co., Ltd.) Temperature
82 and salinity values were linearly interpolated at the longitudinal interval of 0.5° (equivalent to
83 ~50 km) and were averaged vertically every 10 m down to the depth of 780 m.

84 Temperature data at the line of PX37 were obtained by the Scripps High Resolution XBT
85 Program (www-hrx.ucsd.edu). Temperature data were collected by XBT Deep Blue probes

86 (Sippican Inc.), which are nominally rated to 760 m depth, with a maximum horizontal interval
87 of about 60 km. The data were gridded at the vertical interval of 10 m. In March 2005 and
88 November 2006, temperature sections between Honolulu and San Francisco could be obtained
89 simultaneously with that between Japan and Honolulu, i.e., PX40. The data in Junes of 2004,
90 2005, and 2006 are based on the data at PX37 which were obtained within two months of the
91 PX40 observations. In total, the five sections from San Francisco to Japan via Honolulu could be
92 obtained during June 2004–November 2006. Salinity at the XBT data points were determined
93 by averaging the Argo float data within a horizontal distance of 150 km from the XBT points
94 in the database maintained by Japan Argo (www.jamstec.go.jp/ARGO/argoweb/argo). The data
95 were interpolated vertically every 10 m down to the depth of 780 m.

96 To calculate the geostrophic velocity, we set the reference depth to 700 m above the nominal
97 maximum depth of the XBT measurements. This reference depth is located in the layer deeper
98 than the isopycnal depth of $26.5\sigma_\theta$ (kg m^{-3}), i.e., in the lower part of the main thermocline,
99 providing the baroclinic variation of the geostrophic transport relative to 700 m. The volume
100 transport across the WOCE P02 line east of 150°E with the reference depth of 700 dbar, 29.6 Sv
101 ($1 \text{ Sv} = 10^6 \text{ m}^3 \text{ s}^{-1}$), was 12 Sv smaller than 41.5 Sv with the reference depth of 1000 dbar. The
102 difference is considered to be of the same order of magnitude as that of the volume transports at
103 PX37 and PX40 between the reference depths of 700 and 1000 m if the data down to the depth
104 of 1000 m had been obtained.

105 Each transect at PX37 and PX40 was conducted within half a month. Therefore, by inte-
106 grating the geostrophic velocity and the temperature along the lines, the influence of mesoscale
107 eddies on the volume transport and volume transport-averaged temperature of the southward in-
108 terior flow would be canceled out except the region around the western end of the line at 150°E .

109 It should be noted that the error transport caused by eddies around the western artificially fixed
110 end at 150°E is included in the estimated volume transport and volume transport-averaged tem-
111 perature.

112 **3 Results**

113 In this study, the volume transport-averaged temperature, T , is defined as

$$T = \frac{\iint \theta v \, dx dz}{\iint v \, dx dz}, \quad (1)$$

114 where v is the geostrophic velocity normal to the observation lines; θ is the potential tempera-
115 ture; and x and z are the coordinates along the observation line and vertical axis, respectively.
116 The temperatures, T and θ , are in the same unit, °C.

117 By performing the integrations in Eq. (1) over the whole section from Honolulu to San Fran-
118 cisco (PX37) and to 150°E (PX40) above the depth of 700 m, the volume transport-averaged
119 temperature of the baroclinic flow, T_1 , were obtained in Table 1. The values of T_1 at PX37
120 and PX40 are significantly lower than 15.5°C estimated from the P02 line section northward of
121 PX37 and PX40 with the reference depth of 700 dbar. Moreover, it should be noted that the vol-
122 ume transport-averaged temperatures would strongly depend on the adopted reference depth.
123 Using 1000 dbar instead of 700 dbar as the reference depth, the volume transport-averaged
124 temperature at the P02 line is 1°C lower than that with the reference depth of 700 dbar. Accord-
125 ingly, the estimated T_1 from PX37 and PX40 data would have such an order of bias due to the
126 southerly track via Honolulu and the constraint of no motion at 700 m, so that we should focus
127 not on the absolute values but on the relative values.

128 The maximum and minimum values of T_1 were observed to be 14.7°C (November 2006) and
129 13.9°C (March 2005) (Table 1), respectively; in other words, the difference of T_1 maximizes to

130 0.8°C. In order to illustrate the variation of the density structure at the PX37 and PX40 lines
131 that yields the variation of T_1 , the potential density sections are shown in Fig. 2. Contours of the
132 potential density larger than $25.5\sigma_\theta$ commonly shoal eastward, suggesting that the flow in the
133 interior region is directed southward as a whole. Except for March 2005 in Fig. 2b, the seasonal
134 thermocline can be recognized above the depth of about 200 m along the entire lines. In March
135 2005, the seasonal thermocline disappeared associated with the outcrop of the isopycnal of
136 $24.5\sigma_\theta$ in the west of 175°W; at this time, T_1 was observed to be the minimum value.

137 Salinity anomalies on potential density surfaces can be well characterized by a parameter,
138 called the spiciness (Veronis, 1972; Jackett and McDougall, 1985; Flament, 2002). Figure 8
139 prepared by Nagano et al. (2010) shows that the spiciness distributes uniformly on the isopycnal
140 surfaces within the lower part of the main thermocline in the offshore interior region of the
141 subtropical gyre. In this study, the spiciness, π , whose unit is the same as that of the potential
142 density, σ_θ , i.e., kg m^{-3} , was calculated by using the polynomial presented by Flament (2002)
143 (Fig. 3). In the interior region of the subtropical gyre, contours of the spiciness are largely flat
144 in the layer between 23.5 and $26.5\sigma_\theta$ as reported by Nagano et al. (2010), although the contours
145 undulate in the eastern part.

146 Along the west coast of North America, the low-salinity water of subpolar origin, called
147 the shallow salinity-minimum water (SSMW), flows southward (Reid, 1973; Yuan and Talley,
148 1992), but eventually proceeds to the tropical region (Kawabe and Fujio, 2010) as schematically
149 illustrated by dotted curves in Fig. 1. Therefore, the southward transport of the SSMW should
150 be treated as the separated flow transport from the rest interior flow transport of the subtropical
151 gyre. The SSMW was found to be characterized by the subsurface minimum of the spiciness
152 lower than 0.1π (white thick contours) to the east of 135°W, and is distinct from the water

153 occupying the rest interior region.

154 Identifying the SSMW as the water with the spiciness lower than 0.1π above the isopycnal
155 surface of $26\sigma_\theta$, the volume transport of the water, V_{SSM} , and the volume transport-averaged
156 temperature, T_{SSM} , of the SSMW were evaluated as in Table 2. The variation range of V_{SSM} is
157 quite small in comparison with that of V_I , although T_{SSM} is inversely correlated to T_I with the
158 coefficient of -0.88 . Therefore, the variations of the volume transport and volume transport-
159 averaged temperature of the SSMW is not the principal factor to vary the volume transport-
160 averaged temperature of the southward interior flow.

161 To reveal another variation of the interior flow that yields the significant variation of T_I , the
162 remaining volume transport of the interior flow at the lines of PX37 and PX40 after the removal
163 of the SSMW transport is divided into potential density segments with the interval of $0.25\sigma_\theta$
164 (Fig. 4). The primary peak of the net southward volume transport is commonly present in the
165 range between 24.5 and $25.5\sigma_\theta$. Compared with November 2006 (Fig. 4c), the distributions of
166 the volume transport in the other periods are concentrated within narrow density layers such as
167 24.5 – $25.0\sigma_\theta$ in March 2005 (Fig. 4a) and 25.0 – $25.5\sigma_\theta$ in Junes of 2004–2006 (Fig. 4b). Partic-
168 ularly, in every June, the volume transports are similarly allocated. Meanwhile, the distribution
169 in November 2006 (Fig. 4c) is deviated toward the upper layer above approximately $24.0\sigma_\theta$
170 with the secondary peak of the southward volume transport between 23.50 and $23.75\sigma_\theta$.

171 Due to the variation of the volume transport distribution, the net southward transport within
172 the density layer between 24.5 and $26.5\sigma_\theta$ became noticeably smaller in November 2006 than
173 those in the other periods. For neatness sake, the density layer is simply referred to as the mode
174 water layer in this paper because the density range almost includes those adopted to identify
175 the subtropical and central mode waters by Suga and Hanawa (1995) and Suga et al. (1997),

176 respectively. The volume transport in the mode water layer, called V_M , occupies over 60% of
177 the volume transport of the interior flow in the top 700 m, i.e., V_I , so that V_M may be responsible
178 for the variation of T_I . In the shallow layer above $24.5\sigma_\theta$, the southward volume transport is at
179 least up to approximately 5 Sv in November 2006.

180 The variation range of the volume transport in the mode water layer, V_M , (Table 2) is com-
181 parable to that of V_I (Table 1). Moreover, V_M was found to be strongly related to the volume
182 transport-averaged temperature, T_I . As plotted in Fig. 5a, obviously, T_I and V_M are inversely
183 correlated; the correlation coefficient is -0.95 . In other words, the higher proportion of the
184 water flowing in the mode water layer yields the lower T_I . Thus, the volume transport in the
185 mode water layer is principally responsible for the variation of T_I and a potential element affect-
186 ing the climate through the net heat transport of the subtropical gyre. Meanwhile, the volume
187 transport-averaged temperature in the mode water layer, T_M , is less responsible for the variation
188 of T_I than V_M , as indicated by the negative correlation coefficient of -0.71 (Fig. 5b).

189 4 Discussion

190 We estimated the volume transport and volume transport-averaged temperature of the southward
191 interior flow of the North Pacific subtropical gyre on the basis of the five sections from San
192 Francisco to 150°E via Honolulu with the reference depth of 700 m. The volume transport-
193 averaged temperature, T_I , strongly depends on the depth of the reference level, but the obtained
194 values was found to vary with the maximum difference of 0.8°C between November 2006 and
195 March 2005 if the reference depth was fixed to 700 m in all cases. The significant variation of
196 T_I was demonstrated to be associated with that of volume transport in the density layer between
197 24.5 and $26.5\sigma_\theta$, i.e., in the mode water layer. The variation of the volume transport in the
198 density layer is accompanied by the vertical distribution change of the transport. Although, due

199 to the limited vertical range by XBT T-7 and Deep Blue, the absolute values of the volume
200 transport and volume transport-averaged temperature were not fully discussed, the PX37 and
201 PX40 data could supplement the knowledge based on the WOCE P02 data.

202 In this study, the volume transport-averaged temperature of the southward interior flow,
203 which has been treated as an invariable parameter in past studies, was elucidated to vary vigor-
204 ously. Yet, the characteristics of the temporal variation were not clarified sufficiently due to the
205 sparse data in time. The temporal variation should be more addressed in future works by using
206 data obtained more densely in time. The high-resolution hydrographic observations in the inte-
207 rior region such as along the lines of PX37 and PX40 must be continued for more quantitative
208 investigations with a longer duration and more frequent collections per year.

209 **Acknowledgements**

210 This study was carried out as a part of Japan-Hawaii Monitoring Program (JAHMP). The au-
211 thors would like to thank the captain and crew of the T/V *Miyagi-maru* (Miyagi Prefectural
212 Board of Education) for obtaining XBT/XCTD data, and also appreciate Scripps High Resolu-
213 tion XBT/XCTD (HRX) program and Japan Argo team which made the data available in their
214 web sites. Thanks are extended to the editors (Drs. T. Hibiya and T. Suga) and anonymous
215 reviewers for their helpful comments.

216 **References**

217 Bryden, H. and S. Imawaki (2001) Ocean heat transport. In: H. Siedler, J. Church, and J. Gould
218 (eds) *Ocean Circulation and Climate: Observing and Modeling the Global Ocean*, Academic
219 Press, pp. 455–474

- 220 Flament, P. (2002) A state variable for characterizing water masses and their diffusive stability:
221 spiciness. *Prog. Oceanogr.* 54: 493–501
- 222 Jackett, D. R. and T. J. McDougall (1985) An oceanographic variable for the characterization
223 of intrusions and water masses. *Deep-Sea Res.* 32(10): 1195–1207
- 224 Kawabe, M. and S. Fujio (2010) Pacific Ocean circulation based on observation. *J. Oceanogr.*
225 66(3): 389–403
- 226 Nagano, A., K. Ichikawa, H. Ichikawa, M. Konda, and K. Murakami (2009) Synoptic flow
227 structures in the confluence region of the Kuroshio and the Ryukyu Current. *J. Geophys. Res.*
228 114(C06007). doi:10.1029/2008JC005213
- 229 Nagano, A., K. Ichikawa, H. Ichikawa, H. Tomita, H. Tokinaga, and M. Konda (2010) Stable
230 volume and heat transports of the North Pacific subtropical gyre revealed by indentifying
231 the Kuroshio in synoptic hydrography south of Japan. *J. Geophys. Res.* 115(C09002). doi:
232 10.1029/2009JC005747
- 233 Reid, J. L. (1973) The shallow salinity minima of the Pacific Ocean. *Deep-Sea Res.* 20: 51–68
- 234 Roemmich, D., J. Gilson, and B. Cornuelle (2001) Mean and time-varying meridional transport
235 of heat at the tropical/subtropical boundary of the North Pacific Ocean. *J. Geophys. Res.*
236 106 (C5): 8957–8970
- 237 Suga, T. and K. Hanawa (1995) The subtropical mode water circulation in the North Pacific. *J.*
238 *Phys. Oceanogr.* 25: 958–970
- 239 Suga, T., Y. Takei, and K. Hanawa (1997) Thermostad distribution in the North Pacific subtrop-

- 240 ical gyre: The central mode water and the subtropical mode water. *J. Phys. Oceanogr.* 27(1):
241 140–152
- 242 Uehara, H., S. Kizu, K. Hanawa, Y. Yoshikawa, and D. Roemmich (2008) Estimation of heat
243 and freshwater transports in the North Pacific using high-resolution expendable bathyther-
244 mograph data. *J. Geophys. Res.* 113(C02014): doi:10.1029/2002JC004165
- 245 Veronis, G. (1972) On the properties of seawater defined by temperature, salinity, and pressure.
246 *J. Mar. Res.* 30: 227–255
- 247 Yuan, X. and L. D. Talley (1992) Shallow salinity minima in the North Pacific. *J. Phys.*
248 *Oceanogr.* 22: 1302–1316

Table 1: Volume transport, V_I , and the volume transport-averaged temperature, T_I , between 150°E and San Francisco. Positive transports are directed southward.

Year	Month	V_I (Sv)	T_I (°C)
2004	Jun	39.5	14.1
2005	Mar	35.6	13.9
	Jun	37.8	14.1
2006	Jun	34.1	14.4
	Nov	29.2	14.7

Table 2: Volume transport, V_{SSM} , and volume transport-averaged temperature, T_{SSM} , of the SSMW; and volume transport, V_M , and volume transport-averaged temperature, T_M , within the density layer of 24.5–26.5 σ_θ , i.e., the mode water layer. Positive transports are directed southward.

Year	Month	V_{SSM} (Sv)	T_{SSM} (°C)	V_M (Sv)	T_M (°C)
2004	Jun	3.7	9.7	29.8	14.7
2005	Mar	2.6	9.7	32.1	15.4
	Jun	3.0	9.6	29.2	15.0
2006	Jun	2.5	9.1	26.8	14.9
	Nov	2.3	9.3	18.1	14.6

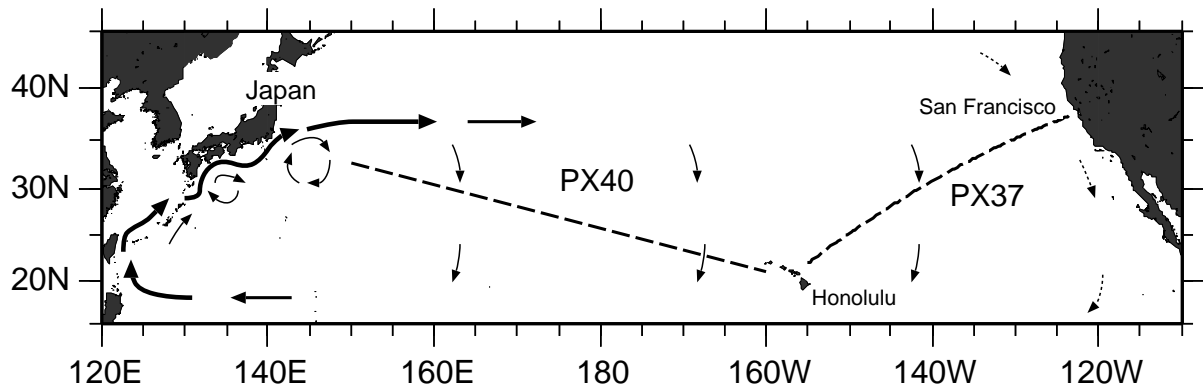


Figure 1: Schematic diagram of the North Pacific subtropical gyre (solid curves with arrows) and flow of the shallow salinity-minimum water (dotted curves with arrows); and the lines of PX37 and PX40 (dashed lines).

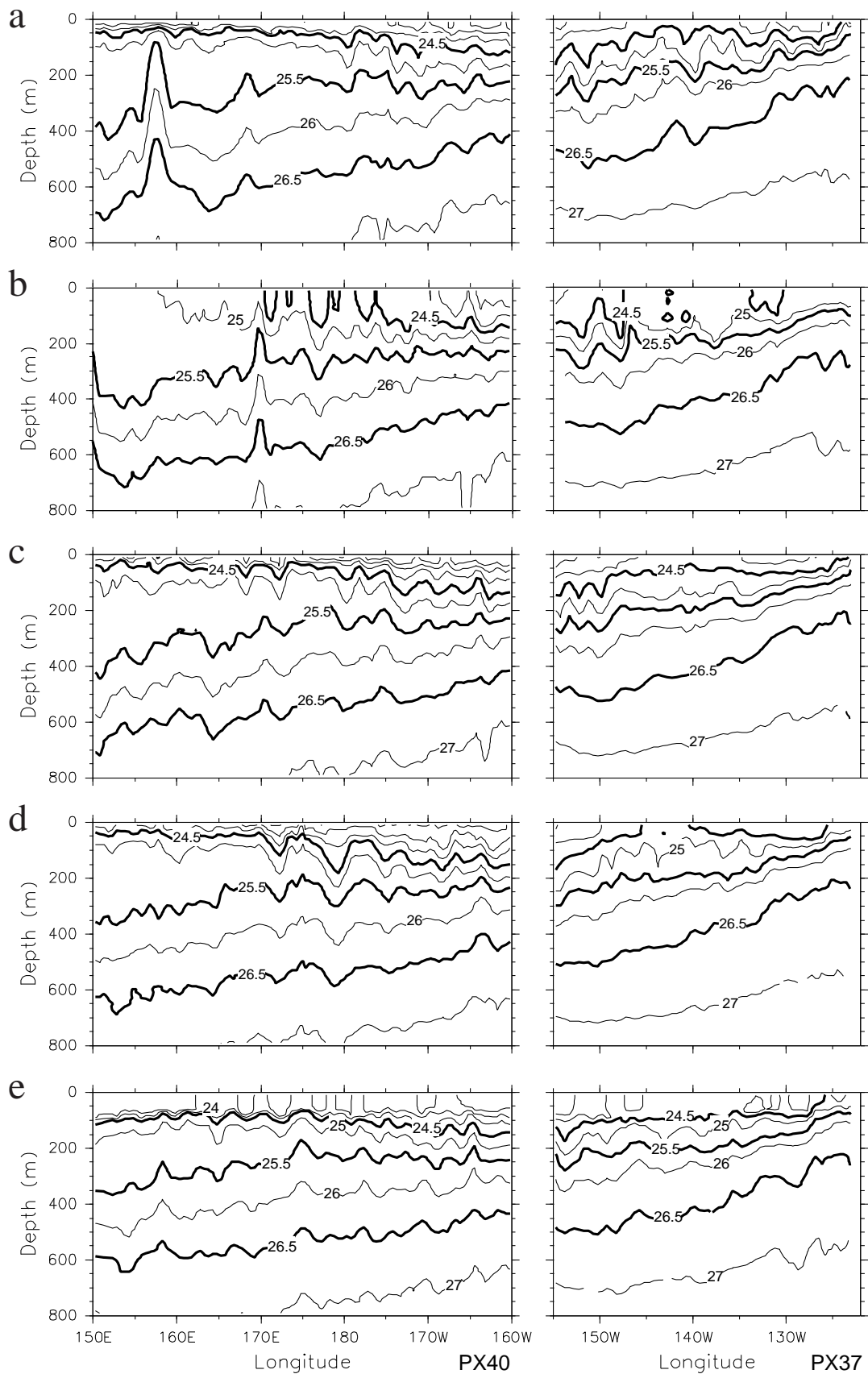


Figure 2: Sections of the potential density σ_θ from San Francisco to 150°E via Honolulu with contour interval of $0.5\sigma_\theta$, thick contours of 24.5 , 25.5 , and $26.5\sigma_\theta$, in (a) June 2004, (b) March 2005, (c) June 2005, (d) June 2006, and (e) November 2006.

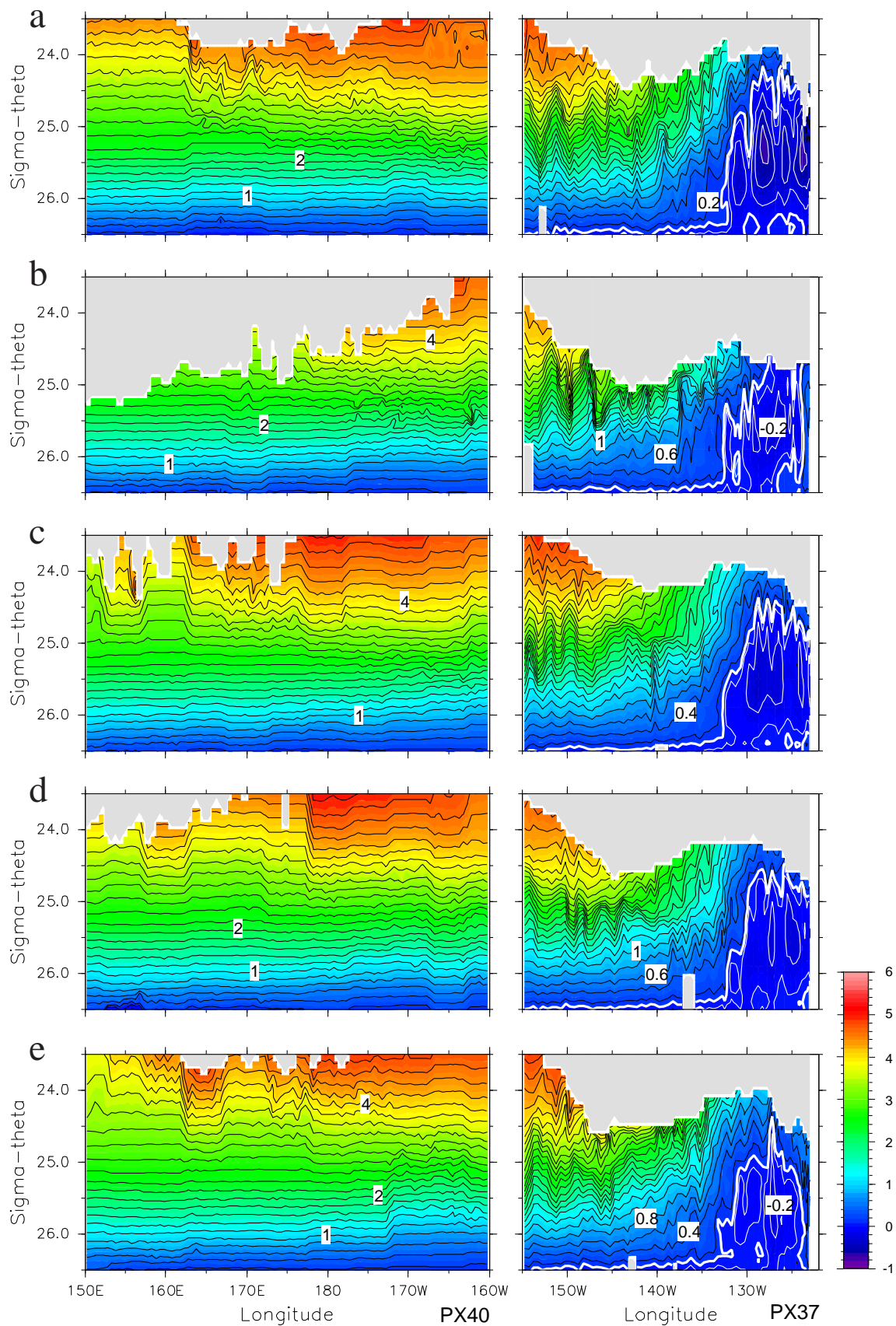


Figure 3: Sections of the spiciness π with respect to the potential density σ_θ from Honolulu to San Francisco (PX37) and to 150°E (PX40) in (a) June 2004, (b) March 2005, (c) June 2005, (d) June 2006, and (e) November 2006. Contour interval is 0.2π and values smaller than 0π is indicated with white thin contours. Only 0.1π is shown with white thick contours.

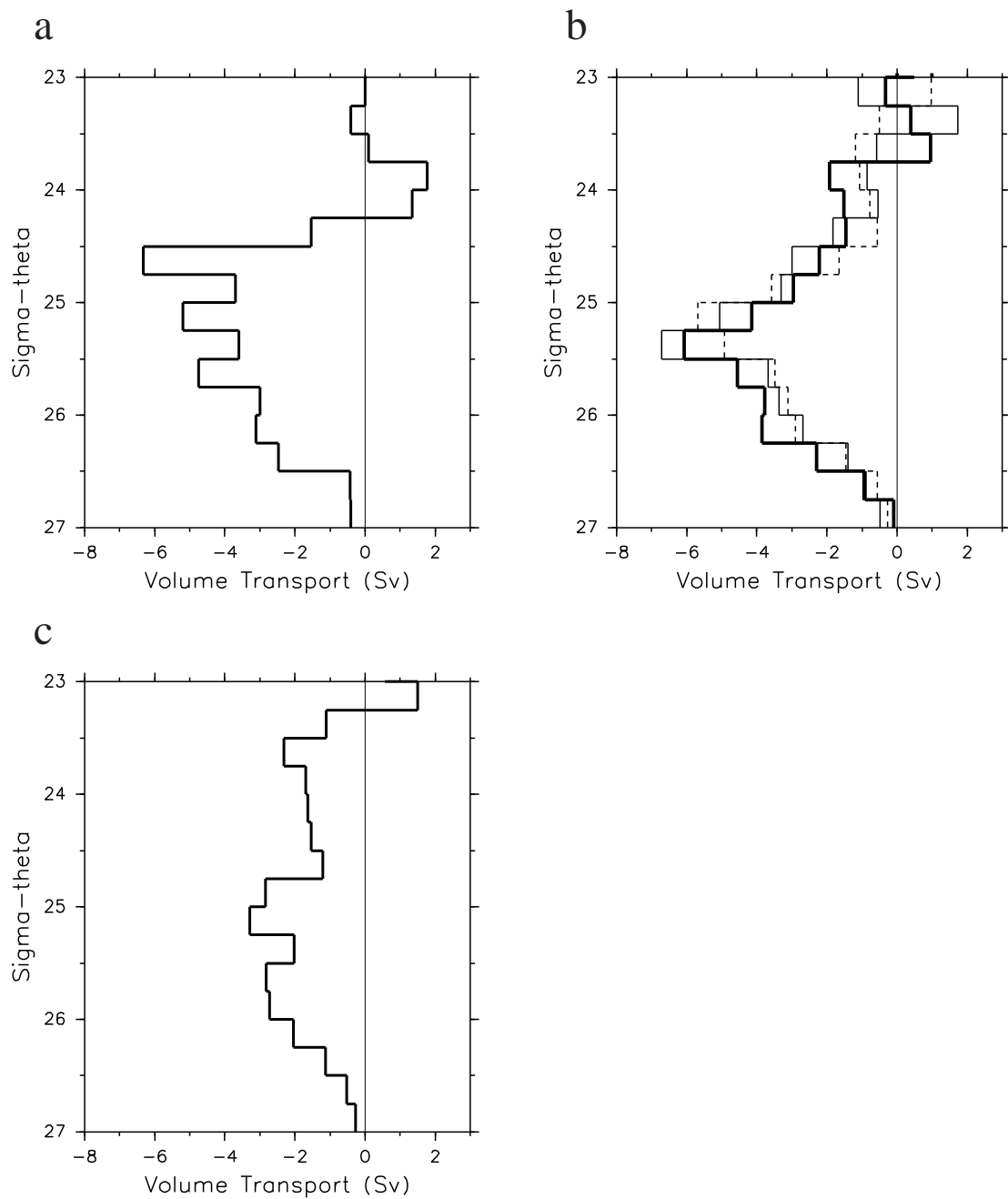


Figure 4: Distributions of the volume transport at the lines of PX37 and PX40 with respect to potential density σ_θ in (a) March 2005, (b) Junes of 2004–2006, and (c) November 2006. Transports were calculated for segments at the interval of $0.25\sigma_\theta$ except the region of the spiciness lower than 0.1π , i.e., the SSMW. Positive values indicate northward volume transports. In (b), values in Junes of 2004, 2005, and 2006 are indicated by thick solid, thin solid, and dashed lines, respectively.

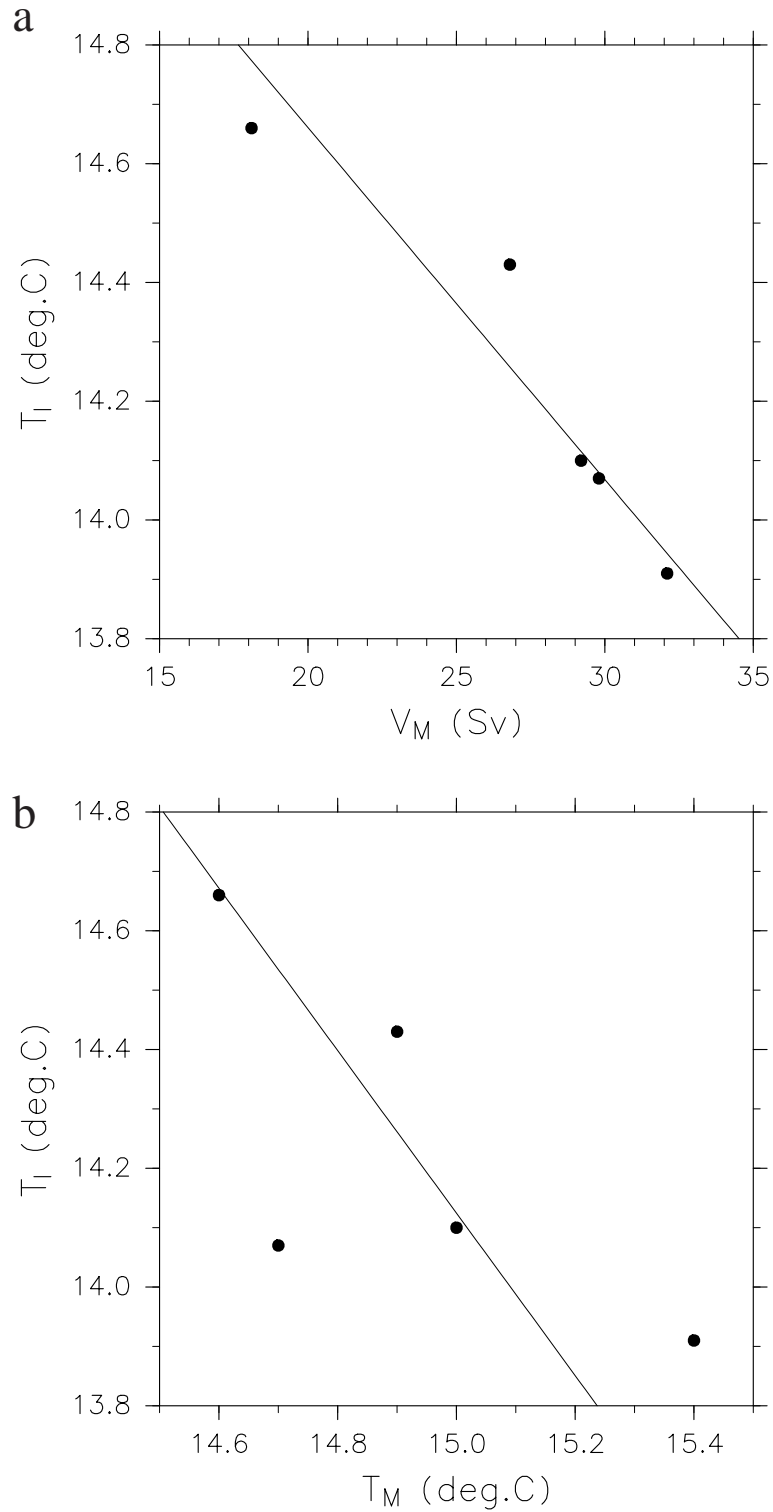


Figure 5: Scatter plots of the volume transport-averaged temperature of the southward interior flow, T_I , versus (a) the volume transport, V_M , and (b) the volume transport-averaged temperature, T_M , for the potential density layer between 24.5 and $26.5\sigma_\theta$, i.e., the mode water layer. Slant solid lines are linear regressions.